LIGHT SCATTERING BY FLUFFY LOW-SILICA Al-Fe-SiO AND Ca-SiO SMOKES OBTAINED BY NON-EQUILIBRIUM VAPOR PHASE CONDENSATION. F. J. M. Rietmeijer[1], E. Hadamcik[2], A. Pun[1], J.-B. Renard[3], J. A. Nuth III[4] and A. C. Levasseur-Regourd[2], [1]Department of Earth and Planetary Sciences, MSC 03-2040, 1-University of New Mexico, Albuquerque NM 87131-0001, USA (email: fransjmr@unm.edu), [2]UPMC Université Paris 06, UMR 7620 (LATMOS/IPSL), BP 3, 91371 Verrières-le-Buisson, France (email: edith.hadamcik@aerov.jussieu.fr), [3] LPCE/CNRS, 3A Avenue de la Recherche Scientifique, 45071 Orléans Cedex2, France, [4]Laboratory of Extraterrestrial Physics, NASA Goddard Space Flight Center, Greenbelt, Maryland, USA

Introduction: The linear polarization of the light scattered off dust particles ejected from active comets, and specifically its dependence upon the phase angle and wavelength of observations, offers an efficient method to characterize their physical properties [1,2]. As part of an ongoing effort using laboratory-produced vapor phase condensed dust analogs (smokes) we report here the results of combined light scattering measurements, scanning electron microscope and analytical transmission electron microscope characterizations of low-silica Al-Fe-SiO and Ca-SiO smokes. So far, it appears that the individual smoke grain compositions have no noticeable effect on the shapes of the light curves [1,2]. Here we emphasize physical properties.

Smoke production and analyses: The smokes were produced in the Condensation Flow Apparatus at the NASA Goddard Space Flight Center that simulated kinetically controlled vapor phase condensation. The samples produced are mixtures of simple-oxide grains (*e.g.* SiO_2) plus binary oxide grains (*e.g.* $CaO{\cdot}SiO_2$) grains with deep metastable eutectic compositions [3]. The experimental conditions and ATEM analyses procedures of used for both smokes are described in [4,5]. The SEM and light scattering measurements of levitating particles are detailed in [1,6]. The light scattering measurements produce bell-shaped phase curves typical of irregular particles with a characteristic phase range of maximum polarization. A negative branch of this curve can be present at phase angles <20°; together these features can be used to extract information on grain size (distribution) and aggregate porosity [1,2].

Observations: The smokes are open, 3-D networks of interconnected necklaces that consist of individual condensate grains that show variable levels of grain-fusion. Simple oxide condensate grains tend to form euhedral mineral grains; grains with intermediate, mixed-oxide compositions will be (sub) spherical.

TEM Analyses. Grains in the Ca-SiO smoke are mostly <120 nm [4]. The condensate grains in Al-Fe-SiO smoke range from 2-25 nm (Table 1); it also contains many randomly scattered dense grain clusters [5].

SEM Analyses. They also show the porous texture of the Ca-SiO smoke and the presence of necklaces of grains of 10-20 nm in size and many platy grains >100 nm (Fig. 1). These platy grains were not seen in such

Table 1: Grain diameters (nm) in the condensed smokes

Range (nm)	Mean (nm)
Ca-SiO smoke (TEM data)	
18-62	33
65-118	84
Low-silica Al-Fe-SiO smoke (TEM data)	
2-25	No data

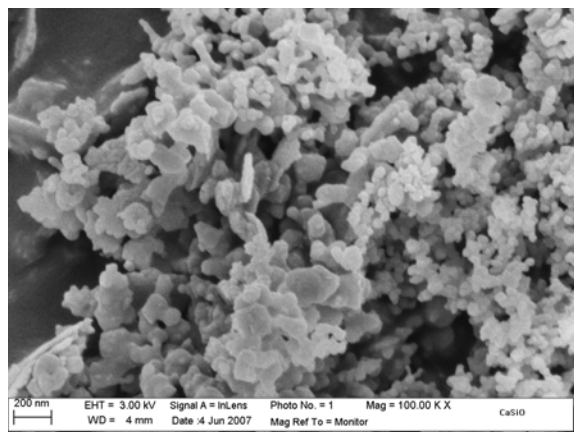

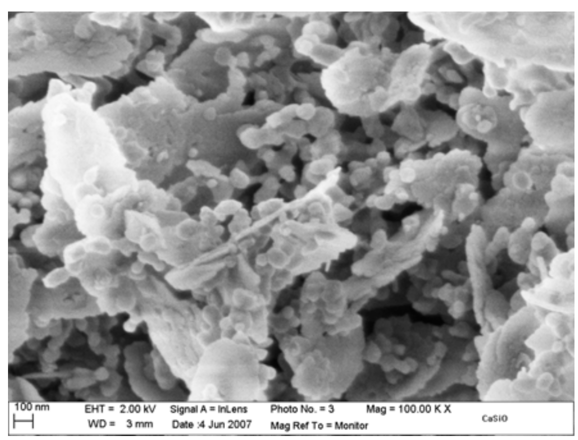

Figure 1: SEM images showing necklaces of grains <100 nm and many platy grains >100 nm (top). The short necklaces are interspersed between the platy grains (bottom).

concentrations during TEM analyses. A similar complementary relationship between TEM and SEM analyses was seen previously [1]. Whereas SEM analyses offer a 'global' view of the smokes, the much smaller samples prepared for TEM analyses tend to favor the fine-grained smoke fractions.

The SEM data for the Al-Fe-SiO smoke show its overall high-porosity with scattered large dense clusters ~50 nm in size sintered spherical grains (Fig. 2). Much larger grains (100nm to 10 microns) are agglomerates of the dense clusters.

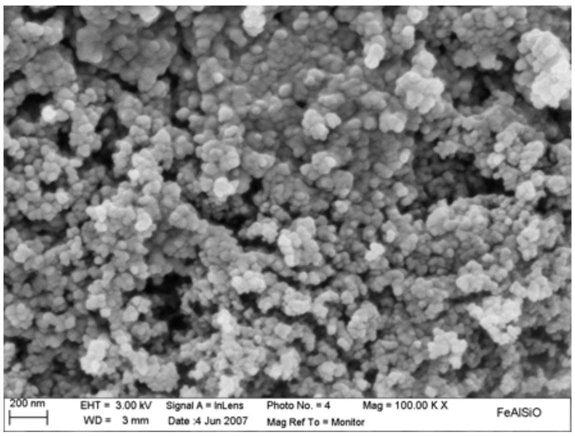

Figure 2: SEM image of the porous Al-Fe-SiO smoke that is dominated by a matrix of small grains.

Light scattering phase curves: Both samples show characteristic bell-shaped curves (Figs 3 & 4). There is no negative branch in the curve of the Ca-SiO smoke (CaO = 35 wt%; SiO_2 = 65 wt%) (Fig. 3). A small negative branch with an inversion angle at 14° ± 5° polarimetric in light scattering phase curve exists for the low-silica Al-Fe-SiO smoke (FeO = 59.3, Al_2O_3 = 25.8, and SiO_2 = 14.9 wt% [5]) (Fig. 4).

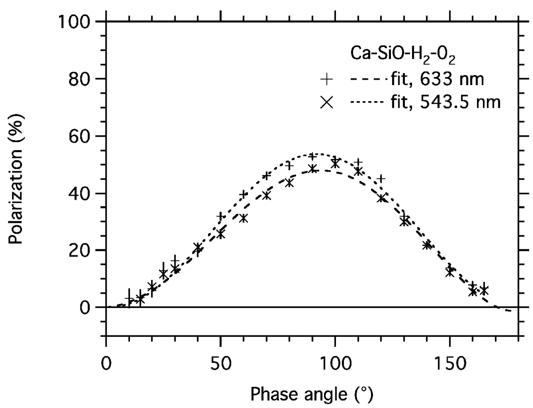

Figure 3: Polarimetric phase curves for the Ca-SiO smoke showing maximum polarization (54 ± 2) % in red light at a phase angle of (95 ± 5)° and (48 ± 2) % in green light at a phase angle of (93 ± 5)°.

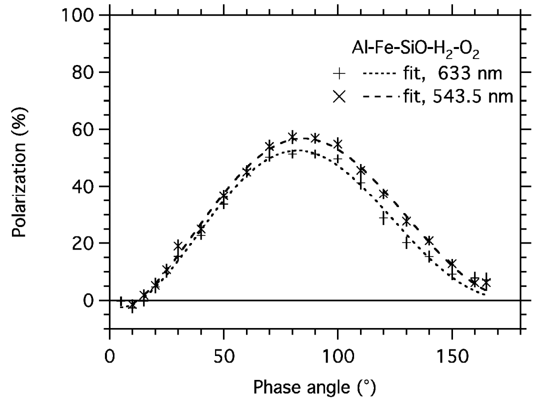

Figure 4: Polarimetric phase curves for the Al-Fe-SiO smoke showing maximum polarization (52 ± 2) % in red light at a phase angle of (86 ± 5)° and (57 ± 2) % in green light at a phase angle of (88 ± 5)°.

The main difference between the two analyzed samples is a positive spectral gradient for Ca-SiO smoke and a small negative spectral gradient for the Fe-containing smoke, possibly due to a greater absorption in green than in red light for this sample. Such a difference was previously also observed in magnesiosilica and ferrosilica smokes [1]. For these samples subtle differences in bulk composition affected their light scattering behavior (producing differences in their complex refractive index).

Conclusions: While Ca-SiO and Al-Fe-SiO materials will be rare in comets their light scattering phase curves closely resemble those for magnesiosilica and ferrosilica smoke mixtures (similar grain sizes and particle size distributions). Cometary particles will also contain carbonaceous compounds simulated by fine-grained carbon black that produces the positive spectral gradient in laboratory spectra and in comet observations [7]. A polarization maximum between 20% and 40% for comet dust requires the presence of micrometer silica grains in the ejected dust population; they are also necessary in analog particles [1,8].

References: [1] Hadamcik E. et al. (2007) *Icarus, 190*, 660-671. [2] Volten H. et al. (2007) *Astron. Astrophys., 470*, 377-386. [3] Nuth J. A. et al. (2002) *Meteoritics & Planet. Sci.*, 37, 1579-1590. [4] Rietmeijer F. J. M. et al. (2008) *Icarus. 195*, 493-503. [5] Rietmeijer F. J. M. et al. (2008) *Chem. Phys Lett., 458*, 355-358. [6] Hadamcik E. et al. (2009) *Light Scattering Rev., vol. 4*, Springer-Praxis, in press. [7] Levasseur-Regourd A.C. and Hadamcik E. (2003) *JQSRT, 79-80*, 903-910. [8] Hadamcik E. et al. (2006) *JQSRT, 100*, 143-156.